Supporting Information

Tong et al. 10.1073/pnas.1009008107

SI Text

SI Materials and Methods. ***DNA construction and protein purification.*** Human cDNA encoding full length CENTA1 (1–374 or 3–370), KIF13B motor domain (4–351), motor+FHA (1–550), KIF13A motor+FHA domains (1–556), FHA domains of KIF13B (440–545), KIF1A (472–598), KIF1C(498–599), KIF14 (813–905), or KIF16B (444–560) were cloned into pET28-MHL (GenBank: EF456735.1) and/or pET28GST-LIC (GenBank: EF456739.1) using the In-Fusion PCR cloning system (Clontech Laboratories). Site-directed mutagenesis was carried out using the QuickChange kit (Stratagene). All proteins were overexpressed in a phage-resistant *Escherichia coli* BL21(DE3) strain harboring the pRARE2 plasmid using the LEX bubbling system (Harbinger Biotechnology and Engineering). His6-tagged proteins were first purified using nickel-nitrilotriacetic acid resin (Qiagen) in batch mode followed by size exclusion chromatography. GST or GST-fused proteins were purified using glutathione-Sepharose beads (GE Healthcare) in phosphate buffered saline (PBS) solution. All protein preparations had >95% purity based on SDS-PAGE, unless otherwise specified. Selenomethionine (SeMet) labeling of CENTA1 was carried out using prepacked M9 SeMet growth media kit (Medicilon), following the manufacturer's instructions.

Crystallization. Native apo-form CENTA1 crystal was grown in 25% PEG3350, 0.2 M ammonium acetate, and 0.1 M Bis-Tris, pH 6.5, in a sitting drop setup. The SeMet labeled CENTA1 crystal used for phasing was grown in 30% PEG3350, 0.2 M ammonium acetate, and 0.1 M Bis-Tris, pH 6.0 in a hanging drop. To grow PIP3-bound CENTA1 complex crystals, purified CENTA1 was mixed with L-α-Phosphatidyl-D-myo-inositol 3,4,5-triphosphate, dioctanoyl (Sigma) in a 1:1 molar ratio right before crystallization. Crystals were grown in 20% PEG3350 and 0.2 M ammonium chloride. The CENTA1/KIF13B-FHA complex was purified from a Superdex-75 column preequlibrated with 20 mM Hepes, pH 7.30 buffer containing 300 mM NaCl, 1 mM tris(2-carboxyethyl)phosphine hydrochloride (TCEP), and 5% glycerol, concentrated, and 2-methyl-1.3-propanediol added to a final concentration of 5% (vol/vol) before crystallization. Crystals were grown in 1.2 M lithium sulfate, 0.1 M sodium citrate, pH 6.0 and 0.5 M ammonium sulfate. It usually took 3–4 weeks for the crystals to grow to a mountable size. Purified CENTA1 and KIF13B-FHA complex was also mixed with PIP3 (Sigma) at 1:1 molar ratio, and 5% (vol/vol) acetone to obtain ternary complex crystals. Ternary complexes were grown in 0.8 M lithium sulfate, 0.5 M ammonium sulfate, 0.1 M sodium citrate, pH 6.0. More experimental details are available on the Structural Genomics Consortium website at http://www.thesgc.org/structures/index.php?terms=centa1.

PIP array assay and differential static light scattering. CENTA1 binding to phosphoinositides was assayed using a PIP array membrane (Echelon Biosciences). Purified His6-tagged CENTA1 (0.5 μg/μL in PBS buffer) was incubated with the membrane at room temperature for 1 h and then probed using anti-His monoclonal antibody (Qiagen) followed by anti-HRP antibody (GE Healthcare) and stained using a tetramethylbenzidine substrate kit (Vector Laboratories). StarGazer (Harbinger Biotechnology and Engineering) was used for differential static light scattering measurement. CENTA1 protein (50 μL, 0.2 mg/mL) was premixed with phosphoinositide stock solutions [D-myo-inositol 1,3,4,5-tetrakisphosphate ammonium salt (IP4, Cat.No. I8635-1mg)] from Sigma, dioctanoyl-PIP3 (Cat.No. 10007764) and dioctanoyl-PI(3,4)P_2 (Cat.No. 10008400) from Cayman Chemicals, dissolved in water to give a final concentration of 4–8 mg/mL) and loaded onto a 384-well plate, covered with mineral oil, and static light scattering was measured at increasing temperatures. The T_{agg} of wild-type and mutant CENTA1 at different IP4 concentrations were fitted using $T_{agg} = T_0 + \Delta T_{max}{}^{*} c/(K + c)$, where c is the concentration of the phosphoinositides, K and T_0 are constants, and ΔT_{max} is the extrapolated maximal possible ΔT_{agg}.

Data collection and crystal structure determination. Diffraction data were collected at the General Medicine and Cancer Institutes Collaborative Access Team (NCI Y1-CO-1020, NIGMS Y1-GM-1104) and Structural Biology Center at the Advanced Photon Source. Use of the Advanced Photon Source was supported by the U.S. Department of Energy, Basic Energy Sciences, Office of Science, under contract No. DE-AC02-06CH11357.) Diffraction images were reduced using the HKL suite (1). Initial phases for apo-CENTA1 were obtained from a selenomethionine derivative in space group $P2_12_12$ using multiple wavelength anomalous diffraction data collected at beamline 19ID and the programs SOLVE and RESOLVE (2). An initial protein model was built using the program O (3). The model was transferred into the monoclinic crystal form using the MOLREP program (4). MOLREP and the CENTA1 coordinates were used also for molecular replacement to solve the complex structures. Initial placement of the FHA domain in the respective complex was performed manually using difference maps and the coordinates of PDB entry 2G1L. ARP/WARP (5) was used for automated rebuilding of the apo-CENTA1 structure and the IP4-bound complex. The models were further rebuilt and refined using the programs COOT (6), PHENIX (7), and REFMAC (8). The model geometry was periodically validated on the MOLPROBITY (9) server. Coordinates were deposited in the PDB (Table S1).

GST-pull down assay. GST or GST-fused proteins immobilized on glutathione-Sepharose beads were incubated with purified binding partners overnight at 4 °C. After three washes in PBS, protein still bound to the glutathione beads was analyzed by SDS-PAGE and stained with Coomassie brilliant blue.

ITC measurement. Purified CENTA1, KIF13B, and their mutants were dialyzed overnight in ITC buffer (25 mM Tris, pH 7.5, 200 mM sodium chloride). KIF13B-FHA or its mutants (about 1 mM) were injected into the sample cell containing about 1.4 mL of 80 μM CENTA1 or its mutants. ITC titrations were performed on a VP-ITC MicroCalorimeter (MicroCal) at 25 °C by using 10 μL injection with a total of 25 injections. Data were fitted with a one binding site model using Microcal Origin software.

Bioinformatics analysis. Protein assembly analysis was carried out using PISA-server (10). All molecular graphics figures were prepared using PyMOL (DeLano Scientific). Electrostatic properties of the protein surfaces were evaluated using adaptive Posson-Boltzmann solver (APBS) (11) and rendered with PyMOL. Structure-based sequence alignments were calculated using PROMALS3D (12) and rendered using ESPript (13). Ligand-protein interaction figures were prepared using LIGPLOT (14).

1. Otwinowski Z, Minor W (1997) Processing of X-ray diffraction data collected in oscillation mode. *Methods Enzymol* 276:307–326.
2. Terwilliger TC (2003) SOLVE and RESOLVE: automated structure solution and density modification. *Methods Enzymol* 374:22–37.
3. Jones TA, Zou JY, Cowan SW, Kjeldgaard M (1991) Improved methods for building protein models in electron density maps and the location of errors in these models. *Acta Crystallogr A* 47:110–119.
4. Vagin A, Teplyakov A (1997) MOLREP: an automated program for molecular replacement. *Journal of Applied Crystallography* 30:1022–1025.
5. Perrakis A, Morris R, Lamzin VS (1999) Automated protein model building combined with iterative structure refinement. *Nat Struct Biol* 6:458–463.
6. Emsley P, Cowtan K (2004) COOT: model-building tools for molecular graphics. *Acta Crystallogr D* 60:2126–2132.
7. Adams PD, et al. (2002) PHENIX: building new software for automated crystallographic structure determination. *Acta Crystallogr D* 58:1948–1954.
8. Murshudov GN, Vagin AA, Dodson EJ (1997) Refinement of macromolecular structures by the maximum-likelihood method. *Acta Crystallogr D* 53:240–255.
9. Davis IW, Murray LW, Richardson JS, Richardson DC (2004) MOLPROBITY: structure validation and all-atom contact analysis for nucleic acids and their complexes. *Nucleic Acids Res* 32:W615–W619.
10. Krissinel E, Henrick K (2007) Inference of macromolecular assemblies from crystalline state. *J Mol Biol* 372:774–797.
11. Baker NA, Sept D, Joseph S, Holst MJ, McCammon JA (2001) Electrostatics of nanosystems: application to microtubules and the ribosome. *Proc Natl Acad Sci USA* 98:10037–10041.
12. Pei J, Kim BH, Grishin NV (2008) PROMALS3D: a tool for multiple protein sequence and structure alignments. *Nucleic Acids Res* 36:2295–2300.
13. Gouet P, Courcelle E, Stuart DI, Metoz F (1999) ESPript: analysis of multiple sequence alignments in PostScript. *Bioinformatics* 15:305–308.
14. Wallace AC, Laskowski RA, Thornton JM (1995) LIGPLOT: a program to generate schematic diagrams of protein-ligand interactions. *Protein Eng* 8:127–134.

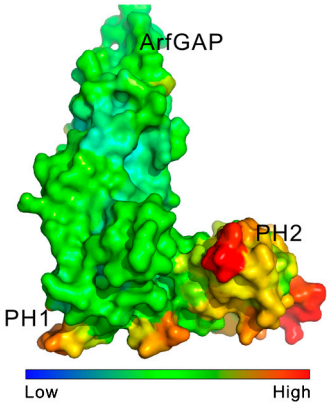

Fig. S1. B-factor of CENTA1. B-factor of the C_α atoms of the apo-form CENTA1 shown on the molecular surface.

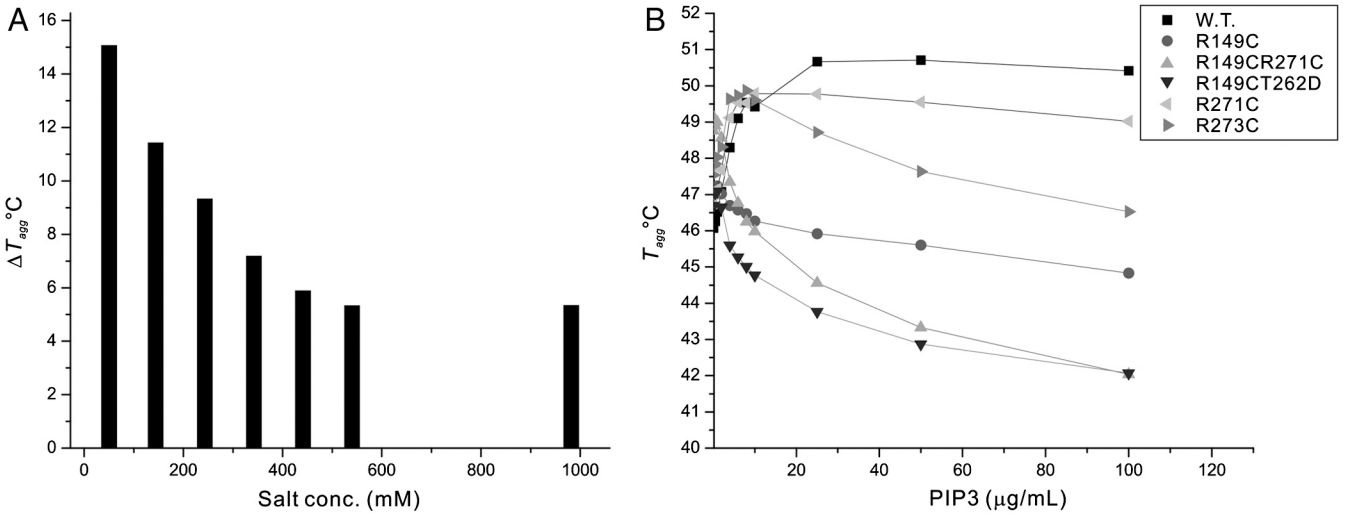

Fig. S2. Differential static light scattering measurement of CENTA1 with phosphatidylinositides. (*A*) Effect of salt concentration on the aggregation temperature T_{agg} for wild-type CENTA1 in the presence of 100 μg/mL IP4. (*B*) Concentration-dependant titration of PIP3 with wild-type and mutant CENTA1.

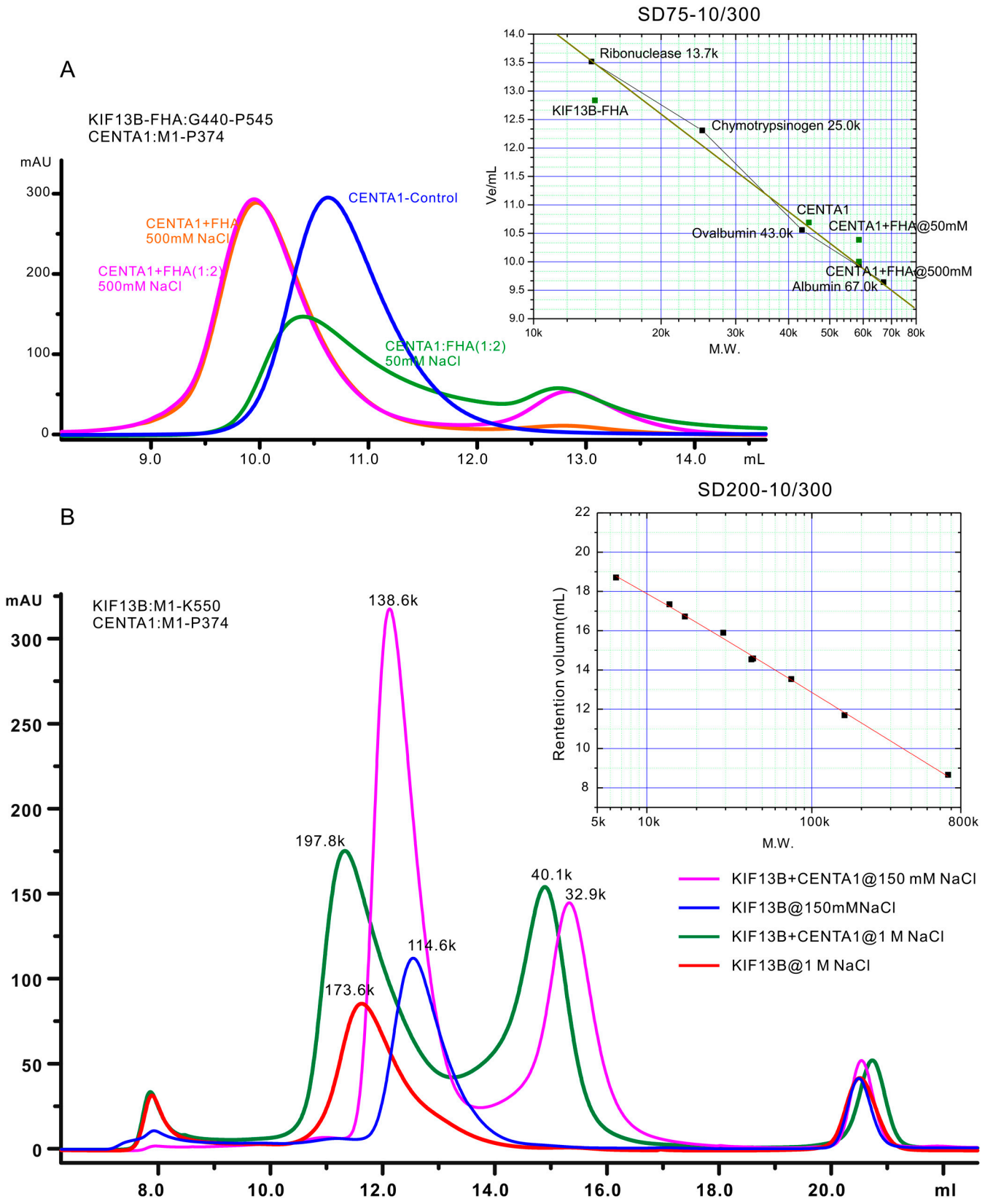

Fig. S3. Gel filtration analysis of the KIF13B and CENTA1 interaction. (*A*) KIF13B-FHA and full length CENTA1 in 20 mM Tris, pH 8.0 buffer containing 1 mM TCEP, 50 mM NaCl or 500 mM NaCl analyzed on SD75-10/300 column (GE Healthcare). (*B*) KIF13B-motor+FHA and full length CENTA1 in 20 mM Tris, pH 8.0 buffer containing 1 mM TCEP, 150 mM NaCl or 1 M NaCl analyzed on a Superdex SD200-10/300 column.

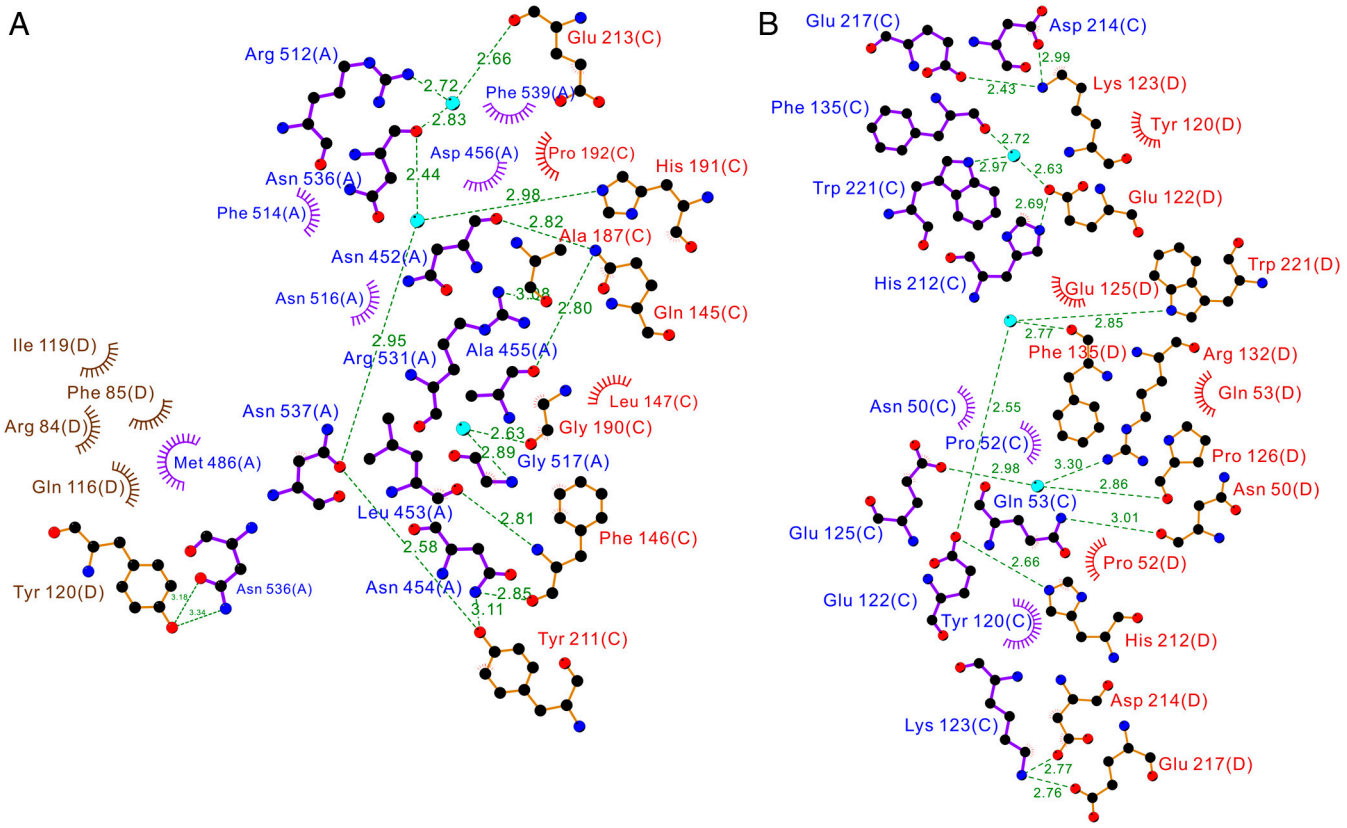

Fig. S4. Ligplot representation of the interaction details of CENTA1 and KIF13B-FHA domain. (*A*) Chain A is KIF13B-FHA. Chain C is the first CENTA1 molecule (PH1 domain). Chain D is the second CENTA1 molecule (ArfGAP domain) (*B*) Interaction between the two CENTA1 molecules (Chains C and D).

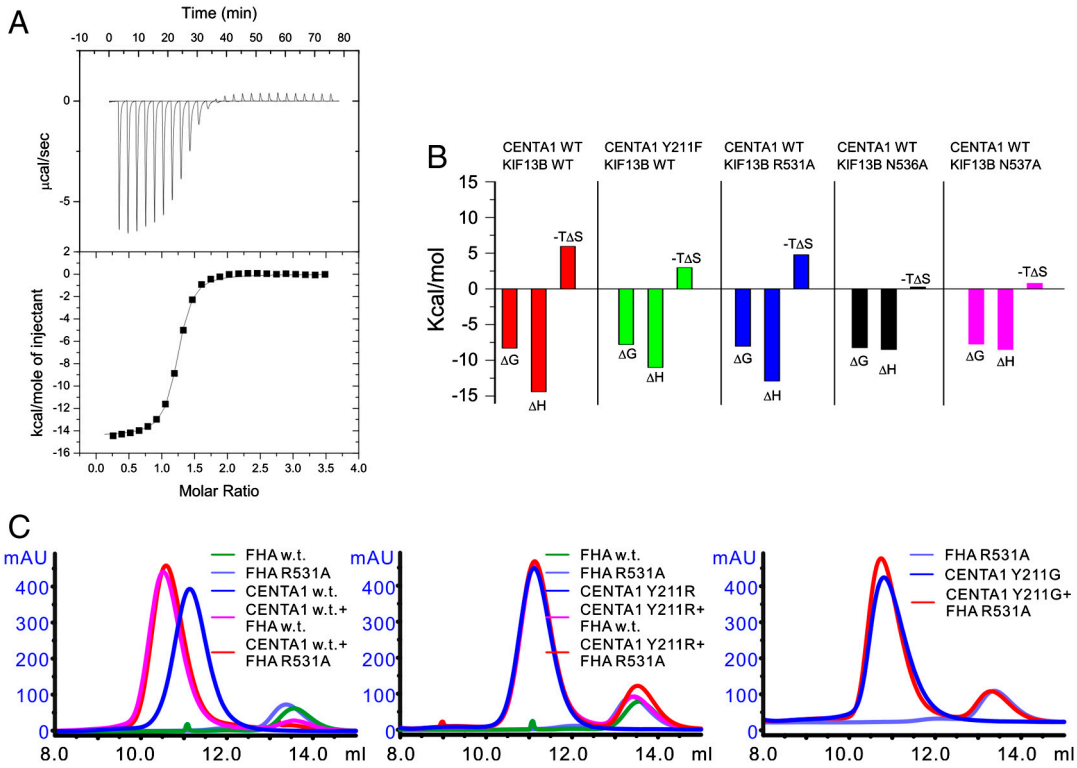

Fig. S5. Characterization of CENTA1/KIF13B-FHA interaction. (*A*) Typical ITC titration curve. (*B*) Summary of the thermodynamics parameters of CENTA1/KIF13B-FHA interaction measured by ITC. (*C*) Size exclusion chromatography analysis of the interaction between CENTA1 and KIF13B-FHA mutants. CENTA1, KIF13B-FHA mutants, or 1:1 molarity ratio of CENTA1/KIF13B-FHA mixture at 100 µM concentration were analyzed on a Superdex-75 10/100 column pre-equilibrated with 50 mM Tris buffer at pH 7.5, containing 500 mM NaCl, 1 mM TCEP. Wild-type CENTA1 could bind to both wild-type KIF13B-FHA and FHA-R531A mutant. Neither CENTA1 Y211R nor Y211G bind to KIF13B-FHA.

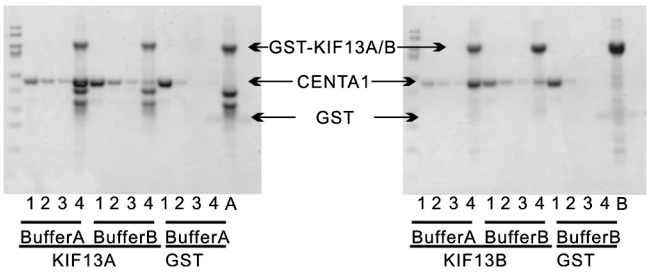

Fig. S6. GST-pull down assay of GST-tagged KIF13 with CENTA1. Purified CENTA1 protein binding with GST or GST-tagged KIF13B motor+FHA proteins. Buffer A, low salt (1X PBS, 0.5 mM TCEP, 0.5% CHAPS); Buffer B, higher salt (1X PBS, 0.5 mM TCEP, 0.5% CHAPS, 500 mM NaCl). Lanes 1–3, flow-through samples after CENTA1 binding, first buffer wash, and second buffer wash. Lane 4, sample still bound to GST beads after washing twice with PBS. Lanes A/B, control samples of KIF13A/B bound to GST beads.

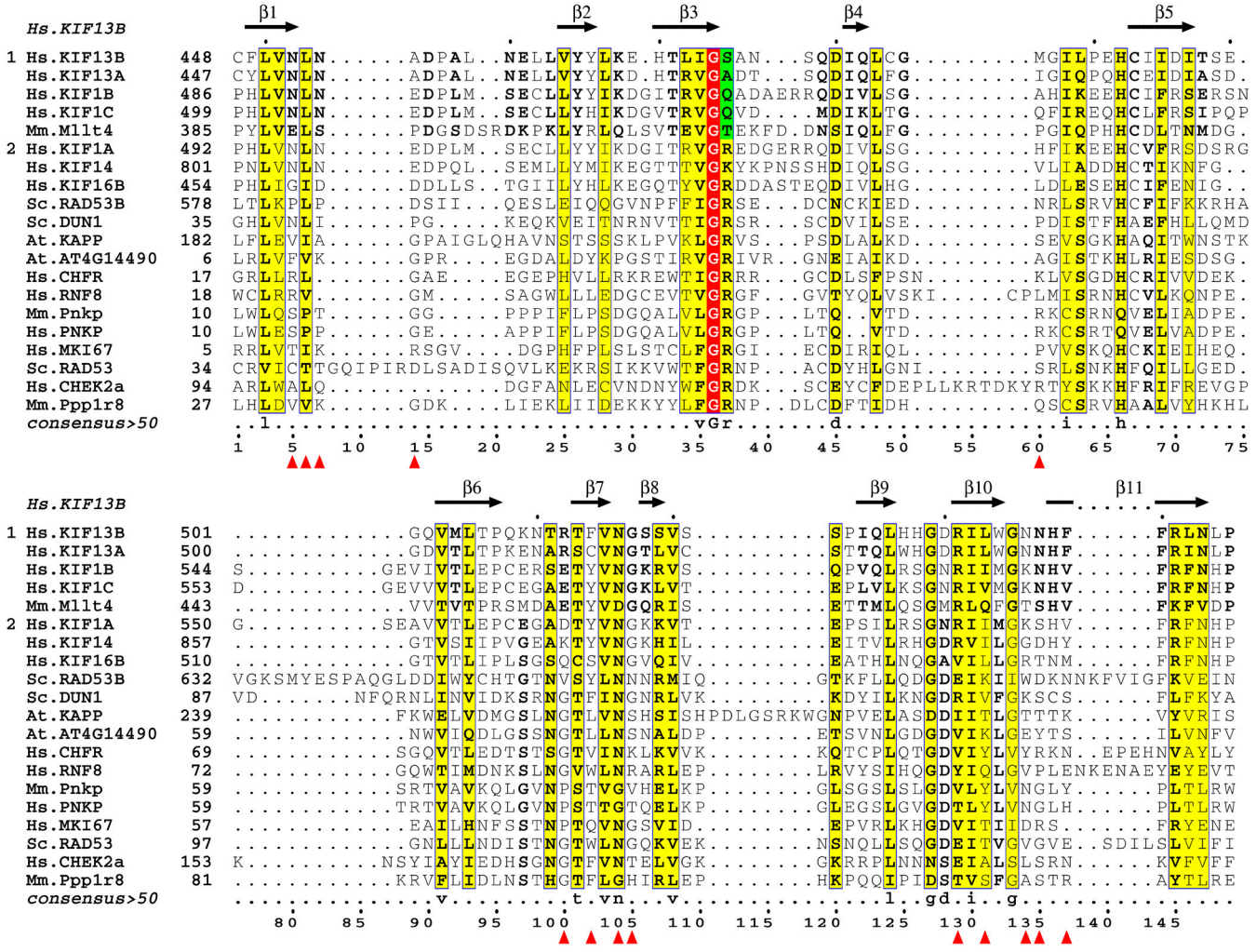

Fig. S7. Structure-based sequence alignment of kinesin-3 family FHA domains with pThr-binding FHA domains. KIF13B-FHA residues interacting with CENTA1 are marked with red triangles. Based on the residue after the invariant glycine (Gly473 in KIF13B), the FHA domains are classified into two groups: group 1 contains a non-K/R residue (green), group 2 contains a lysine or an arginine. All the pThr-binding FHA domains selected have deposited structure coordinates in the protein data bank.

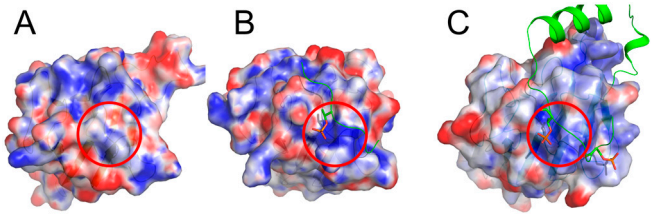

Fig. S8 Surface electrostatic potential comparison of KIF13B-FHA domain with pThr-binding FHA domains. (*A*) Structure of the FHA domain in the CENTA1/KIF13B complex (PDB:3FM8). (*B*) Structure of *Mycobacterium tuberculosis* EmbR FHA domain bound with pThr peptide (PDB:2FF4). (*C*) Structure of Ki76 complexed with hNFIK peptide (PDB: 2AFF). Electrostatic potential was calculated using APBS and rendered by PyMOL. Phosphorylated residues of the peptides are shown in sticks.

Table S1. Crystallographic data and refinement statistics of CENTA1 and its complex structures

	native	w/IP4	w/FHA	w/FHA,IP4
Protein Data Bank code	3FEH	3LJU	3FM8	3MDB
Diffraction data				
Beamline	23ID-B	19ID	19ID	23ID-B
Radiation wavelength (Å)	0.96863	0.97918	0.97918	0.97625
Oscillation range (°)	600 × 0.3	0.5 × 240	187 × 0.5	360 × 0.5
Space group	C2	$P2_12_12_1$	$P4_12_12$	$P4_12_12$
Unit cell dimensions (a, b, c; Å)	118.06	51.73	115.63	115.80
	52.38	66.41	115.63	115.80
	65.02	127.22	189.29	189.27
β (°)	106.45			
No. of copies in asymmetric unit	1	1	2	2
Resolution range (Å)*	50 - 1.90 (1.97 - 1.90)	50.00 - 1.70 (1.73 - 1.70)	20 - 2.30 (2.38 - 2.30)	30.00 - 2.95 (3.06 - 2.95)
Unique reflections	27,553 (1,607)	48,266 (2,338)	57,550 (5,574)	27,800 (2,716)
Data completeness (%)	91.1 (53.8)	98.8 (97.3)	99.7 (98.3)	100.0 (100.0)
R_{sym} (%)†	8.3 (37.7)	10.8 (47.6)	8.0 (73.9)	13.9 (95.7)
Redundancy	3.1 (1.7)	4.3 (2.8)	7.1 (5.3)	14.6 (14.7)
Average I/σ_I	20.2 (1.9)	18.2 (1.7)	25.3 (2.4)	26.2 (3.5)
Refinement statistics				
Resolution limits for refinement (Å)	37.05 - 1.90	20.00 - 1.70	19.86 - 2.30	29.44 - 2.95
R_{work} (%)‡ / R_{free} (%)	20.9/25.5	19.1/23.1	23.1/27.2	22.5/27.7
No. of atoms				
Protein	2,857	3,069	7,162	7,066
Ligand/ion	1	52	17	30
Water	136	294	134	0
R.m.s. deviation from ideal				
bond length (Å)	0.016	0.16	0.014	0.011
bond angles (°)	1.5	1.5	1.3	1.2
Average B-factors, Å^2				
Protein	31.7	15.6	44.0	61.0
Ligand/ion	24.3	15.9	46.8	65.8
Water	32.9	23.0	35.5	N/A
Ramachandran plot (%)				
Most favored	93.6	92.9	92.0	90.3
Additional allowed	5.8	6.8	7.5	9.0
Generously allowed	0.3	0.0	0.3	0.4
Disallowed	0.3	0.3	0.3	0.3

*Numbers in parentheses are for outer shell.

†$R_{sym} = \sum |I-\langle I\rangle| / \sum I$.

‡$R_{work} = \sum ||F_o|-|F_c|| / \sum |F_o|$, where F_o and F_c are the observed and calculated structure factors, respectively. R_{free} was calculated as R_{work} by using 3.8% of the data selected in thin resolution shells with SFTOO.

Table S2. Comparison of the rmsd (Å) of the C_α atoms in individual domains and in the overall structure of CENTA1

Structure pair	ArfGAP*,†	PH1*	PH2*	Overall*
w/IP4 vs. apo	0.189	0.379	0.530	0.451
w/FHA vs. apo	0.170	0.371	0.279	0.738
Ternary vs. apo	0.194	0.308	0.311	0.804
Ternary vs. w/IP4	0.280	0.234	0.434	0.860
Ternary vs. w/FHA	0.130	0.168	0.297	0.192

*ArfGAP: residues 12–119, PH1: residues 131–238, PH2: residues 253–359, overall: residues included in all three individual domains.

†When bound with KIF13B-FHA domain, the N terminus of the CENTA1 molecule has unusual displacement, which was probably caused by crystal packing, thus the first 11 residues are excluded in rmsd calculation.

Table S3. Isothermal titration calorimetry measurement of the interaction between CENTA1 and KIF13B-FHA

	CENTA1/KIF13B	CENTA1 (Y211F)/ KIF13B	CENTA1/KIF13B (R531A)	CENTA1/KIF13B (N536A)	CENTA1/ KIF13B (N357A)
ΔG (kcal·mol^{-1})	−8.3	−7.9	−8.0	−8.2	−7.7
ΔH (kcal·mol^{-1})	−14.4	−11.0	−12.9	−8.5	−8.5
$-T\Delta S$ (kcal·mol^{-1})	6.0	3.0	4.8	0.3	0.8
K_d (μM)	0.8	1.7	1.2	1.0	2.2

Table S4. Summary of GST-pull down assay of kinesin-3 family members with centaurin α

	GST-CENTA1	GST
KIF13B motor	+	+
KIF13B motor+FHA	+	+
KIF13B-FHA	+	−
KIF1B-FHA	−	−
KIF1C-FHA	−	−
KIF14-FHA	−	−
KIF16B-FHA	−	−

	GST-KIF13A motor+FHA	GST-KIF13B motor+FHA	GST
CENTA1	+	+	−
CENTA2	+	+	+